EFFECT OF FRICTION STIR-WELDING TOOL PIN GEOMETRY ON THE CHARACTERISTICS OF AL-CU JOINTS

UDC:621.791.051
Original scientific paper https://doi.org/10.18485/aeletters.2023.8.2.3

Hammad T. Elmetwally[1], Mostafa A. Abdelhafiz[1], M. N. El-Sheikh[1], Mahmoud E. Abdullah[1*]

[1]Mechanical Department, Faculty of Technology and Education, Beni-Suef University, Beni-Suef 62511, Egypt

Abstract:
Friction stir welding (FSW) is considered to be a solid-state welding technique that is suitable well for joining copper and aluminium sheets. The current experimental study focused on the influence of pin geometry on the micro-structural and mechanical characteristics of such joints. An aluminium sheet was welded to a copper sheet at a constant rotational speed of 1280 rpm and a traverse speed of 16 mm/min. The welding tool was made from W302 steel with four different pin profiles: straight cylindrical, tapered, triangular, and squared. When the squared pin was utilized, the optimum joint was produced as the specimen prepared from this joint had a defect-free structure and a tensile strength of 107.2 MPa (80% of the aluminium strength). On the other hand, the pin with a triangular profile was utilized to determine the minimum characteristics, and the specimens' structures revealed dislocations, separations, and cracking in copper particles inside the aluminium matrix. The microhardness trend is consistent across all specimens. Moreover, specimens welded using squared and cylindrical pin tools have the maximum hardness values obtained at the stir zone of the copper side. The inspection of fractured surfaces showed well mixing between aluminium and copper as well as ductile fracture when a squared pin tool was used while it showed a combination of ductile fracture and brittle fracture for the specimen welded with a triangular pin tool. Based on this study, the use of the squared pin tool gives the most favourable results compared with other pin profiles.

ARTICLE HISTORY
Received: 8 March 2023
Revised: 3 May 2023
Accepted: 6 June 2023
Published: 30 June 2023

KEYWORDS
FSW, dissimilar joint, pin geometry, joint strength, microstructure, peak temperature, ductile-brittle fracture

1. INTRODUCTION

The Friction Stir Welding (FSW) method is widely recognized as a crucial technique for joining metals and alloys that possess ultra-oxidation layers during the welding process through fusion techniques. For this reason, FSW is used for welding aluminium, copper, steel, and dissimilar joints; it can also be used underwater [1-4]. FSW procedure includes heating the ends of two parts of the joint to a temperature below the minimum melting point of the base metals [5,6]. This feature gave FSW an advantage over fusion techniques for welding many metals, such as welding aluminium, copper, and titanium alloys [7-9]. Welding different metals, such as aluminium and copper, are highly important for reducing weight by replacing copper with aluminium, saving welding costs, and considering the safety factor of welded joints [10,11]. Many industrial applications, such as electrical applications in power plants, tend to reduce production costs when minimized copper usage as it was replaced by aluminium. Several previous works studied the effects of FSW process

*CONTACT: M.E. Abdullah, e-mail: bsu_mahmoud@techedu.bsu.edu.eg

parameters to obtain the best welding conditions of the FSW process. Esmaeili et al. [12] studied the effect of welding parameters, such as tool rotational speed and tool offset, on the microstructure and mechanical properties of pure aluminium and brass. They obtained the maximum efficiency at a rotational speed of 450 rpm with a 1.6 mm tool offset that produces proper material flow due to the presence of an intermetallic layer at the interface in addition to crack deflection by the occurrence of a lamellar composite structure in the stir zone. Mehta & Badheka [13] reviewed the effect of welding parameters on material flow, microstructure, and welding defects. It can be seen that the use of copper and aluminium joints welded by FSW is still limited due to the low mechanical properties and formation of IMCs in large amounts. Imperfections, such as fragmental defects, voids, pores, and cracks, are commonly found in dissimilar Cu–Al FSW systems which are formed due to improper process parameters. The effect of single pass and dual pass on the microstructure of different aluminium series has been studied [9]. It was concluded that a significant growth in the grain size during the second pass reduces the hardness at the heat-affected zone and; consequently, reduces the joint strength by 4.8%. Dhanesh Babu et al. [14] studied the effect of pin geometry on the heat generation, mechanical properties, and microstructure of AZ80A Mg alloy. It was found that the cylindrical pin gave a high welding temperature approximately 83%. In contrast, the triangular pin profile gave a lower value of 79%. Although the high temperature is an effective factor in friction stir welding, the optimum grain size appeared at a temperature of 81:82 % using a Taper cylindrical pin profile. Celik & Cakir [15] studied the influence of welding conditions, i.e. rotation speeds, tool traverse speeds, and tool position on the welding properties of aluminium and copper. They carried out the optimum welding strength at a welding pitch 66.5 rev/mm, and 1 mm tool offset. Msomi & Mabuwa [16] evaluate the position of material as a welding parameter, which is put on the advancing side once and other on the retreating side on fatigue strength during FSW/FSP. They found that the location of strong material put in the advancing side refinement welding stir zone, in contrast, weak material put in the advancing side has an undesirable effect on welding efficiency. The effect of tool offset on the stir zone properties of copper plates has been investigated [17-19]. The tool pin was taper shape; the tool offset was taken 0, 0.3, and 0.6 mm from the center tool axis. It was concluded that the tool offset has significant welding parameters which enhance the hardness and welding strength besides grain refinement in the stir zone at an optimum tool offset of 0.3 mm. García-Navarro et al. [20] evaluate the effect of tool rotational speed and tool travelling speed on both welding temperature and electrical properties of welded joints of aluminium and copper; the welding tool was a threaded cylindrical pin with a flat shoulder. The workpiece fixation for all welded specimens, the copper put on the advancing side, and the aluminium put on the retreating side. The results carried that the electrical resistivity increased with decreasing the tool travelling speed and the higher value of temperature recorded occurred at a welding pitch of 65 rev/ mm. Ghiasvand et al. [21] evaluate the impact of tool offset, pin offset, and material position of different aluminium series on welding temperature. They carried out the pin offset as the main effective welding parameter recorded high welding temperature. Bokov et al. [22] studied the impact of pin shape on the thermal cycle for welding aluminium and steel sheets. The steel is put on the advantage side and the aluminium is put on the retreating side. They found that 15:26% of the heat generated during the friction welding process was generated by the tool pin. Elmetwally et al. [23] suggest an optimization between tool rotational speed and tool travelling speed to improve the mechanical and microstructural properties for welding aluminium to copper using the FSW process. The results have shown that the maximum strength of the welded joint was carried at lower travelling speeds and higher rotational speeds. Chupradit et al. [24] studied the effect of pin geometry on heat generation and mechanical working during the FSW process. It was found that the mechanical working increased with increasing the pin tilt angle. In addition, rising in the welding temperature was observed as increasing the contact area between the tool and the workpiece. Recent works developed a mathematical model to estimate the effect of pin geometry on the heat generated during the FSW process [25,26].

FSW process is still under development. Many articles deal with FSW process parameters, such as rotational speed, traverse speed, tool offset, tool-tilt angle, positions of aluminium and copper sheets, and shoulder shape. Limited articles studied the effect of pin geometry on the mechanical and microstructural properties of the Al-Cu joints. Therefore, the present work aimed to

investigate the impact of pin shape (as a category of tool geometry) on the mechanical and microstructural properties of FSW process used to weld copper with aluminium. The present study includes the effect of pin shape on the heating cycle and thus on the mechanical and microstructural properties.

2. THE EXPERIMENTAL

2.1 Materials and tools

Pure copper and aluminium (as received) with 3 mm in thickness plates were used as base metals for the joints. The chemical composition of the base metals is laboratory checked and given in Table 1 and in Table 2. The mechanical properties of the base metals are determined using tensile and hardness tests and given in Table 3. Four FSW tools made from W302 steel are machined to their final dimensions and heat treated to achieve the required hardness value (50-52 HRC) to retain its surface shape and prevent pin corrosion. The FSW tool is designed with a flat shoulder shape and different pin geometries (shapes). The selected pin geometries (as shown in Fig. 1) were cylindrical, taper, straight triangle, and straight square. For all shapes, the pin length was 2.4 mm i.e., 80% of base metal thickness.

Table 1. Chemical composition of aluminium (as received)

Element	Si	Fe	Co	Zn	Pb
Wt.%	0.02	0.54	0.013	0.02	0.031
Element	Sn	V	Ti	Other	Al
Wt.%	0.04	0.015	0.024	0.031	99.3

Table 2. Chemical composition of copper (as received)

Element	Fe	Sn	Pb	S	Zn
Wt.%	0.11	0.099	0.016	0.01	1.73
Element	Al	C	Cr	Other	Cu
Wt.%	0.04	0.01	0.015	0.07	97.9

Table 3. Mechanical properties of the base materials

Property	Yield strength (MPa)	Ultimate Tensile strength (MPa)	E %	Hardness (HV)
Al (as received)	85	134	6	48
Cu (as received)	90	241	54	129

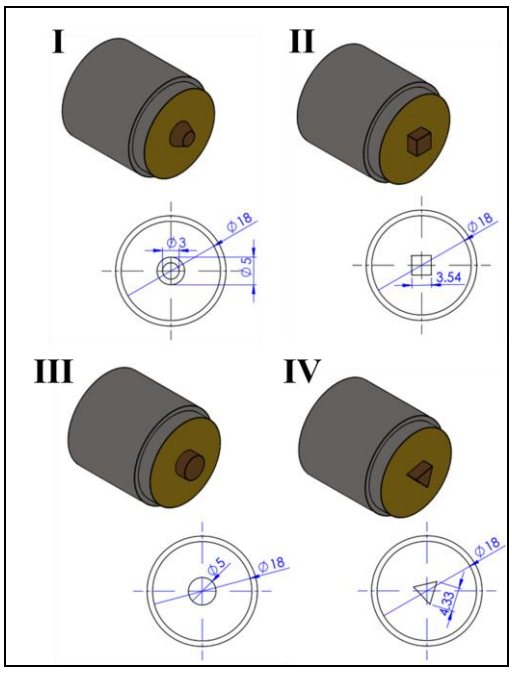

Fig. 1. Pin Configurations and Design; I) Taper, II) Square, III) cylindrical, and IV) Triangle

2.2 Procedures and tests

Rectangular strips with dimensions of 75x120 mm are cut from (as received) aluminium and copper sheets. The aluminium and copper strips are fixed together on a fixture device. The fixture device and the welding tool were held at a milling machine milko-r35 as shown in Fig. 2a. Based on literature work, the tool tilt angle was selected as 2 degrees for all welded specimens [13,18,27]. A travelling speed of 16 mm/min and rotational speed of 1280 rpm is selected for welding all specimens according to the best results and recommendations from research [23]. The temperature was measured and checked using a thermocouple type K and an IR camera (BOSH^{TM}, thermos detector GIS 1000 °C). Each of the measuring instruments has been calibrated (±1 °C). The thermocouple bulb (sensor) was fixed with the help of Epoxy adhesive on the copper side at the middle of the welding pass at 0.5 mm depth. The thermocouple was connected to the Avometer to obtain the temperature value directly, which was recorded every 5 seconds. The welding temperature was measured and checked by using a calibrated thermocouple. During the welding process, the copper strip was put on the advancing side (AS) and the aluminium strip was put on the retreating side (RS). After the welding process was done, the tensile, hardness and microstructure samples were cut from the welded joint as shown in Fig. 2b.

The tensile samples were designed according to ASTM-E8M standard. The tensile test was done on a universal testing machine QUASAR 100-VAV201 with a capacity of 100 KN. The microhardness was measured at a direction perpendicular to the welding direction and carried out on a Vickers testing machine, VMH tester model number 1600-4981, with a dwell time of 15 s and 500 gf. The tensile test results are conducted by using microstructural analysis using an optical microscope and scanning electron microscope. The microstructural specimens were ground, polished, and chemically etched before the microstructural analysis. The sanding process was performed on the cross-section area perpendicular to the welding direction then polished with 5µm and 2µm diamond paste and etched by using an etching solution that consists of 190 ml H_2O, 5 ml HNO_3, 3 ml HCl, and 2 ml HF acid for the aluminium side and 25 ml H_2O, 10 ml H_2O_2, and 25 ml NH_4OH for the copper side. The etched surfaces were examined using an optical microscope (type: Olympus PMG 3). The fracture behaviour of the tensile fractured surfaces was evaluated via scanning electron microscope (SEM), "type: Carl Zeiss-SIGMA 1500VP".

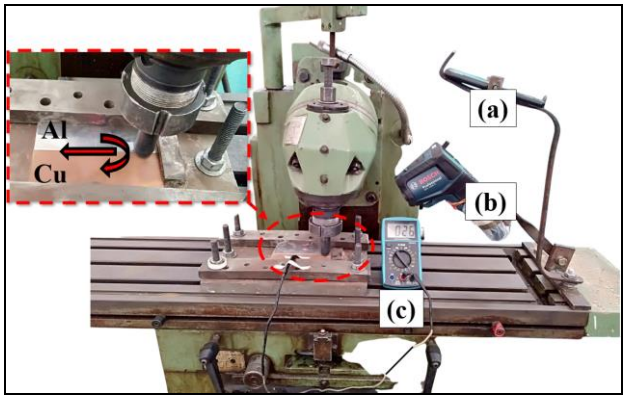

Fig. 2a. FSW process setup; (a) Recorder temperature, (b) IR camera, and (c) Thermocouple

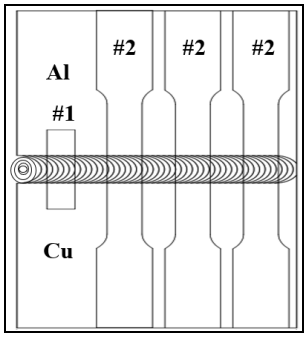

Fig. 2b. Schematic view of FSW specimen design; (#1) Hardness and Microstructure sample, (#2) Tensile test samples

3. RESULTS AND DISCUSSION

3.1 Morphology and Microstructural analysis

The surface morphology of the optimum and worst Al-Cu joints can be seen in Fig 3. The optimum surface was obtained when the joint was welded using a squared pin tool (Fig. 3a). The welded surface of such joint displays no grooves, holes, or surface imperfections, with a few flashes on the copper side. Other pin profiles, such as triangular pins, display longitudinal fractures and flashing flaws (Fig. 3b).

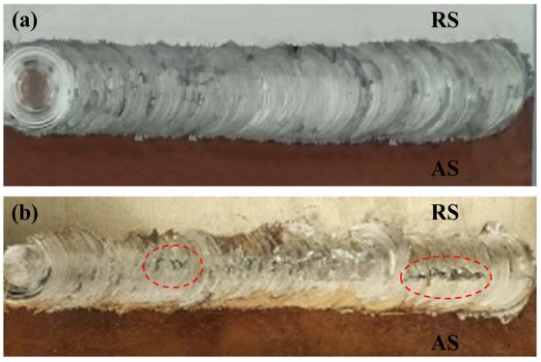

Fig. 3. The appearance of the joint surface welded using: (a) squared pin, (b) triangular pin

Fig. 4 depicts an EDX study at point on the interface line between Cu and Al sides of a specimen welded using a squared pin tool, demonstrating excellent mixing between Al and Cu.

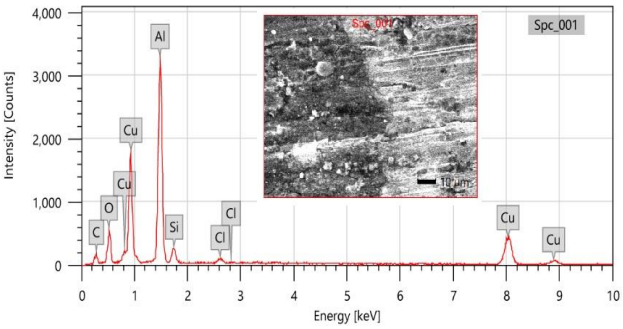

Fig. 4. EDX analysis of SZ of the specimen welded by squared pin (at the interface between Al and Cu)

Fig. 5 displays optical images of square pin configurations at various zones, whereas Fig. 6 provides optical images of the stir zone for the triangular pin. The heat-affected zone (HAZ) structure of Al side is shown in Fig. 5a, while Fig. 5b presents the structure of the interface between the stirring zone (SZ) and the thermal-mechanical affected zone (TMAZ) in the Al side. In the squared pin case, there is a good mixing of aluminium and

copper in the stir zone; little Cu bits are noted in the stir zone on the aluminium side and get greater towards the end of the stir zone near the copper side (Fig. 5c and 5d). On the copper side, copper particles are small in the stir zone (SZ), elongated and compressed in the thermal-mechanical affected zone (TMAZ), and eventually bigger in the heat-affected zone (as shown in Fig. 5e and 5f).

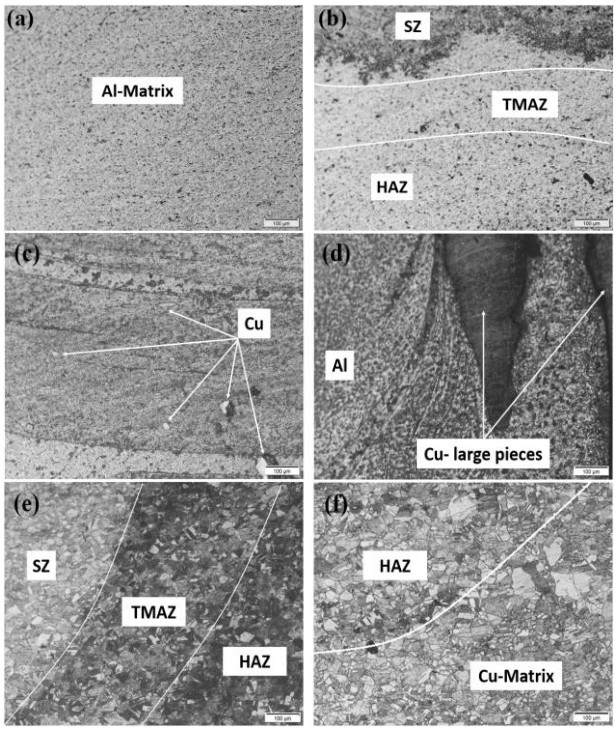

Fig. 5. Microstructural images of squared pin profile: (a) Al-matrix, (b) Al-side SZ&HAZ & TMAZ, (c) RS of SZ, (d) nugget zone, (e) Cu-side SZ, TMAZ and HAZ, (f) Cu matrix

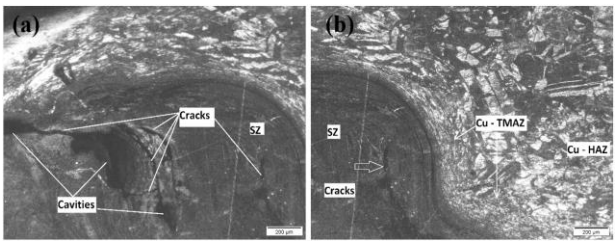

Fig. 6. Microstructural images of triangular pin profile: (a) SZ of Cu side, (b) TMAZ & HAZ of Cu side

Fig. 7a and 7b show SEM images of the aluminium side's HAZ and TMAZ. The microstructure of the HAZ and the TMAZ shows the presence of fine particles which indicates dynamic recrystallization. The stirring motion raises the temperature to the recrystallization point of aluminium, resulting in the formation of a new and tiny particle. Recrystallization occurred entirely in the HAZ and only partially in the TMAZ of the aluminium side. These findings are consistent with prior research [20,21]. The stirring motion in the stir zone ensures proper mixing of fine aluminium particles and coarse copper pieces/particles (Fig. 5c). On the copper side, small copper particles are seen in the stir zone. These particles grow to become coarser and harder in the TMAZ and HAZ, as illustrated in Fig. 5e. The microstructure produced in the specimen welded by the triangular pin tool is completely different; surface defects grow inside the stirring zone, as shown in Fig. 6a and 6b, and these defects include cavities and cross and longitudinal cracks, which are expected due to the impulse action of the triangular profile. Fig. 7 shows the SEM images for the microstructure of different zones. The fine particle structure of the heat-affected zone for the squared pin is given in Fig. 7a while a mixed structure between the Al particles and Cu pieces at the TMAZ is shown in Fig. 7b. The SEM images of the flaws formed in the stir zone when the triangular pin used are shown in Fig. 7c, 7d and 7e. These flaws include large voids and cavities, as indicated in Fig. 7c, separation and fractures in certain copper particles (Fig. 7d), and agglomerations of fractured copper layers inside the aluminium matrix (Fig. 7e).

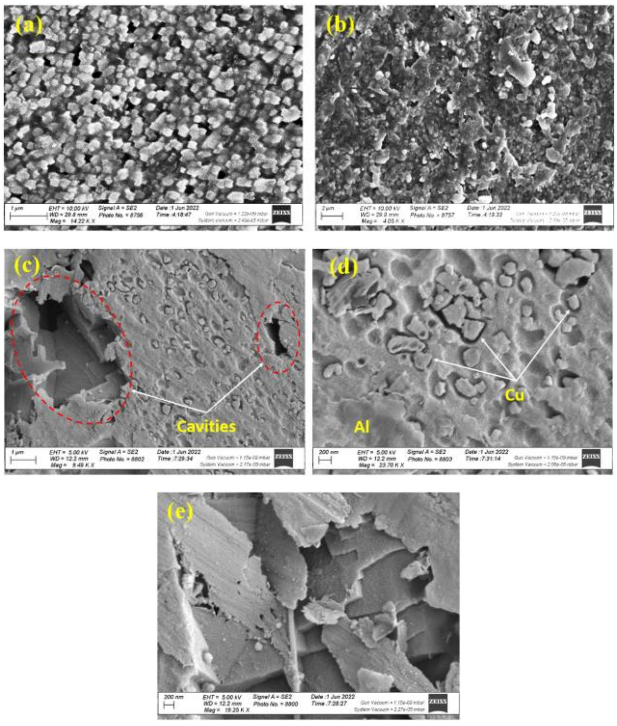

Fig. 7. SEM images for the microstructure of different zones of Al-Cu joint welded by FSW for: (a) squared pin tool at HAZ (b) squared pin at TMAZ, (c), (d) and (e) defects at stir zone of the triangular pin; cavities and dislocation (c), fracture in Cu particles (d), and fracture and separation of Cu layer (e)

3.2 Thermal cycle

The differences in transient temperature for each pin profile were studied and presented in Fig. 8. In general, the temperature-time shapes were similar for all pin profiles. The thermal cycle includes the heating region starting as the tool engaged in the workpiece until the transient temperature reached its peak value followed by the cooling region which continued until the tool leaves the workpiece. The maximum heating rate was 1.573 °C/s for the square profile while the minimum heating rate was 1.151 °C/s for the triangle profile. On the other hand, the maximum cooling rate was found as -1.205 °C/s for the square profile while the minimum cooling rate was -0.832 °C/s for the triangle profile also. The peak temperatures were 316 °C, 288 °C, 255 °C, and 231 °C for square, tapered, cylindrical, and triangle profiles respectively. The contact area between the tool profile and the workpiece (as the friction influence) plays a significant factor in evaluating the amount of transferred heating energy. Square and cylindrical profiles have the maximum contacted area and then the tapered profile while the triangle profile has the minimum contacted area (see Table 4).

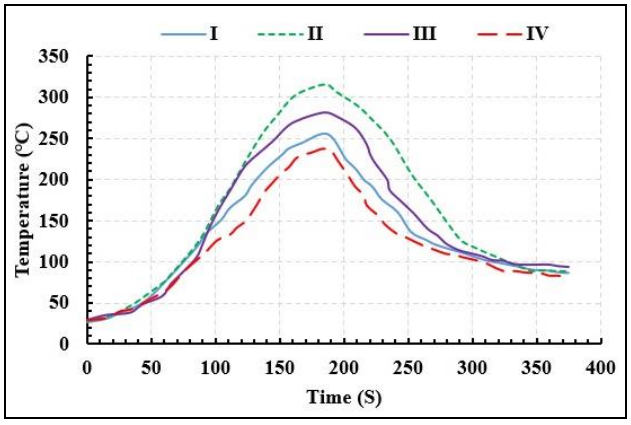

Fig. 8. Thermal cycle for different pin profiles

Table 4. Contacted area and peak temperature for different pin profiles

Tool	Symbol	Total contact Area (mm^2)	Peak Temperature (°C)
Taper	I	274.58	255
Square	II	288.41	316
Cylindrical	III	292.17	282
Triangle	IV	285.65	238

3.3 Mechanical properties

3.3.1 Joint strength

The tensile test is employed to determine joint strength for each pin profile, and the results are shown in Fig. 9.

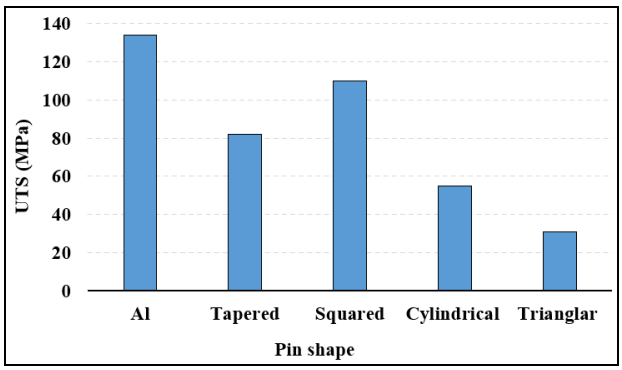

Fig. 9. Joint strength in MPa versus pin shape

The joint strength varies significantly depending on the tool pin profile. The largest strength was achieved in the square pin case, which was 80% aluminium strength, followed by the tapered pin, which was 60% aluminium strength. Since the minimum strength value is 22.5% of aluminium strength, the pin shape has a significant impact on joint efficiency. Due to the friction effect, the material in front of the tool is heated, agitated, and pushed behind the tool, while the forward motion extrudes another layer around the tool [21]. The pin with flat faces (square and triangular) is associated with eccentricity which causes incompressible material to pass around the pin profile [28] and make multiple pulses for each tool rotation which swept the material around the tool [29]. The stirred material produces dynamic swept which largely differ according to tool profile [28,30]. The maximum dynamic swept was found for triangular pin and then for the squared pin. The ratio between the dynamic swept material volume to the static material volume is 2.3, 1.56, 1.09, and 1 for triangular, squared, tapered, and cylindrical pin profiles respectively [28-30]. The higher pulsating effect and dynamic swept of squared pin produce higher localized plastic deformation which maximizes the heat generated during the welding process and therefore improves the joint strength and efficiency. Although the higher values of dynamic swept of the specimen welded by triangular pin profile, number of defects (as shown in Fig. 5) produced through stirring action caused a weak joint and lower strength value.

Khodaverdizadeh et al. [31] showed that the recrystallized grain size in the SZ is the main reason for improving the mechanical properties of the specimen welded by squared pin over specimen welded by other pin profile; however, the grain size in the SZ is finer in the case of squared profile. On contrary, samples welded using other pin profiles have weaker properties because of their coarse grains. Improvement in mechanical properties, when squared pin profile, was used over other pin profiles are in agreement with other references [7,28-30].

3.3.2 Joint hardness

The hardness of the joint is measured perpendicular to the welding line closest to the top surface, and the results for various tool profiles are shown in Fig. 10. The hardness decreased slightly in the stir zone (SZ) around the welding line and reached a minimum value at 2 mm from the datum toward the copper side before suddenly increasing to a maximum value at 3-4 mm from the welding line around the circumference or pin edge closer to the copper side's thermal-mechanical affected zone (TMAZ). The hardness value decreases as a result of stirring action, which softens the particles and raises strain amount in these places, followed by strain hardening in the area close the pin surface. The peak hardness corresponded to the peak temperature, i.e. the maximum hardness obtained for the squared and tapered pin configuration and the minimum hardness obtained for the triangular and cylindrical pin configuration, indicating the effect of welding temperature in hardening the grains in the stir zone. The lowest hardness number for all specimens is less than aluminium hardness while the maximum hardness number is greater than copper hardness. Thermal exposure induces a significant softening effect, reducing the hardness of the SZ. The substantial grain refinement generated by welding with a square pin profile; on the other hand, enhances the hardness of the SZ [19]. The hardness test results can show the failure location and form of the tensile test, which occurs in the stir zone but near to the aluminium side and seems to be a ductile fracture, as detailed in the following item.

3.3.3 Joint Fracture

The fracture was generated on the joints' retreating side (aluminium) due to variations in the temperature distribution and flow of the material in the weld zone, with associated hardness distribution and strained area. Fig. 11 depicts the fracture surface of joints welded with triangular and squared cylindrical pin shapes. By micro void coalescence, both the samples had ductile fracture morphology. Nonetheless, the triangular pin profile joint (Fig. 11a and 11b) displays some cleavage type fracture mode and bigger voids, as well as the presence of intermetallic components (IMCs) indicating poorer ductility of the joint. In the case of the joint welded employing square pin profile (Fig. 11c and 11d); however, fully dimple-like fracture mechanism and lack of huge voids are seen, indicating better ductility of the joint. Shear and deep dimples in Fig. 11c and 11d indicate the existence of a ductile fracture.

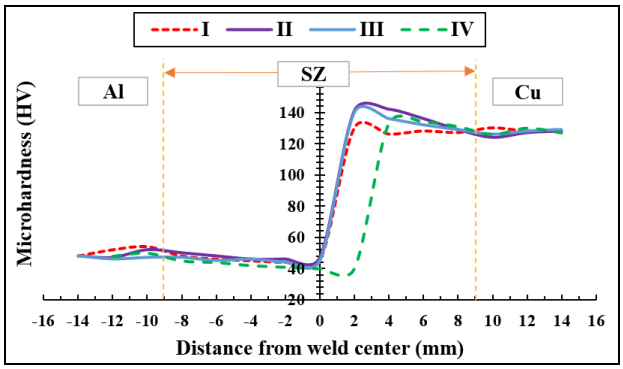

Fig. 10. Micro-hardness of welded joints at different pin profiles

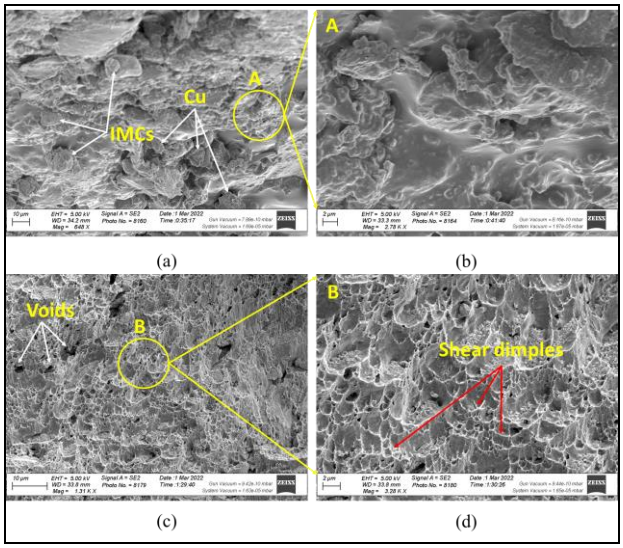

Fig. 11. SEM images for the fractured surfaces of tensile specimen welded by: triangular pin profile (a and b) and squared pin profile (c and d)

Phases of the worst specimen in mechanical and microstructural properties are examined via XRD. The resulted XRD pattern is given in Fig. 12. The XRD pattern demonstrates the existence of intermetallic components (IMCs) in the form of

Al_2Cu at the cracked surface. These IMCs are almost harder than the neighbours' particles and layers [32]. As IMCs founded, joint defects were initiated and grew in these areas.

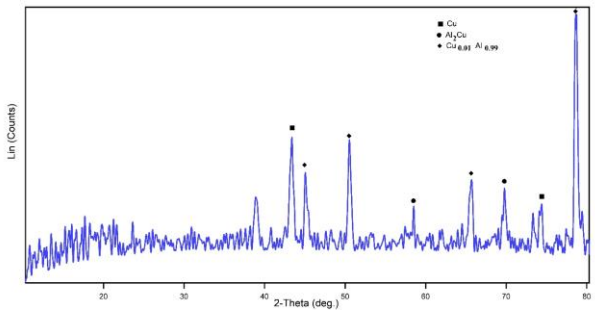

Fig. 12. XRD pattern of Al-Cu joint welded by triangular pin tool

4. CONCLUSIONS

Straight cylindrical, tapered, triangular, and squared profiles are utilized to properly weld the Al-Cu joints. Optical and scanning electron microscopes were employed to study the microstructure of the welded joints; mechanical characteristics of the welded specimen were measured using tensile and hardness tests, and fractured surfaces of the tensile test specimens were evaluated via SEM. Based on the findings of this study, the following conclusions may be drawn:

1. Using a squared pin profile resulted in practically free flaw structure and good appearance welded surfaces. Other pin profiles created a poor structure with extensive voids, agglomerations, cavities, separations, and fractures of copper particles.
2. Under the effect of dynamic swept due to unbalanced stirring action for squared pin profile, particle softening, and dynamic recrystallization are produced and improved the mechanical properties in which the joint strength reached about 80% of the matrix strength. The triangular pin profile's stirring action produced higher values of dynamic swept and internal defects which cause lower mechanical properties.
3. The highest hardness values achieved while utilizing a squared pin or tapered pin are compatible with the measured temperatures. The maximum hardness is found in the SZ around the pin edge/circumference on the Cu side owing to strain hardening, whereas the minimum hardness is found at the zero-line due to material softening caused by stirring action.
4. When a squared pin profile is utilized, ductile fracture occurs, but a mixed brittle-ductile fracture occurs owing to the presence of flaws or intermetallic components when a triangular pin profile is employed. The fracture happened towards the end of the aluminium side's SZ.

ACKNOWLEDGMENT

The authors extend their thanks and appreciation to the technical staff, Faculty of Technology and Education, Beni-Suef University, Egypt.

REFERENCES

[1] A. Heidarzadeh, S. Mironov, R. Kaibyshev, G. Çam, A. Simar, A. Gerlich, F. Khodabakhshi, A. Mostafaei, D.P. Field, J.D. Robson, A. Deschamps, Friction stir welding/processing of metals and alloys: A comprehensive review on microstructural evolution. *Progress in Materials Science*, 117, 2021: 100752. https://doi.org/10.1016/j.pmatsci.2020.100752

[2] S. Sirohi, S.M. Pandey, A. Świerczyńska, G. Rogalski, N. Kumar, M. Landowski, D. Fydrych, C. Pandey, Microstructure and Mechanical Properties of Combined GTAW and SMAW Dissimilar Welded Joints between Inconel 718 and 304L Austenitic Stainless Steel. *Metals*, 13(1), 2022: 14. https://doi.org/10.3390/met13010014

[3] M.M.Z. Ahmed, M.M.E. Seleman, D. Fydrych, G. Çam, Friction Stir Welding of Aluminum in the Aerospace Industry: The Current Progress and State-of-the-Art Review. *Materials*, 16(8), 2023: 2971. https://doi.org/10.3390/ma16082971

[4] H.I. Khalaf, R. Al-Sabur, M. E. Abdullah, A. Kubit, H.A. Derazkola, Effects of Underwater Friction Stir Welding Heat Generation on Residual Stress of AA6068-T6 Aluminum Alloy. *Materials*, 15(6), 2022: 2223. https://doi.org/10.3390/ma15062223

[5] V.P. Singh, S.K. Patel, B. Kuriachen, Mechanical and microstructural properties evolutions of various alloys welded through cooling assisted friction-stir welding: A review. *Intermetallics*, 133, 2021: 107122. https://doi.org/10.1016/j.intermet.2021.107122

[6] G.K. Padhy, C.S. Wu, S. Gao, Friction stir based welding and processing technologies - processes, parameters, microstructures and applications: A review. *Journal of Materials Science and Technology*, 34(1), 2018: 1–38. https://doi.org/10.1016/j.jmst.2017.11.029

[7] V.P. Singh, S.K. Patel, A. Ranjan, B. Kuriachen, Recent research progress in solid state friction-stir welding of aluminium–magnesium alloys: a critical review. *Journal of Materials Research and Technology*, 9(3), 2020: 6217–6256. https://doi.org/10.1016/j.jmrt.2020.01.008

[8] B. Singh, K.K. Saxena, P. Singhal, T.C. Joshi, Role of Various Tool Pin Profiles in Friction Stir Welding of AA2024 Alloys. *Journal of Materials Engineering and Performance*, 30, 2021: 8606–8615. https://doi.org/10.1007/s11665-021-06017-3

[9] K. Gangwar, M. Ramulu, Friction stir welding of titanium alloys: A review. *Materials & Design*, 141, 2018: 230–255. https://doi.org/10.1016/j.matdes.2017.12.033

[10] T. Dursun, C. Soutis, Recent developments in advanced aircraft aluminium alloys. *Materials & Design (1980-2015)*, 56, 2014: 862–871. https://doi.org/10.1016/j.matdes.2013.12.002

[11] Q. Zhang, W. Gong, W. Liu, Microstructure and mechanical properties of dissimilar Al–Cu joints by friction stir welding. *Transactions of Nonferrous Metals Society of China*, 25(6), 2015: 1779–1786. https://doi.org/10.1016/S1003-6326(15)63783-9

[12] A. Esmaeili, M.K.B. Givi, H.R.Z. Rajani, A metallurgical and mechanical study on dissimilar Friction Stir welding of aluminum 1050 to brass (CuZn30). *Materials Science and Engineering: A*, 528(22-23), 2011: 7093–7102. https://doi.org/10.1016/j.msea.2011.06.004

[13] K.P. Mehta, V.J. Badheka, A Review on Dissimilar Friction Stir Welding of Copper to Aluminum: Process, Properties, and Variants. *Materials and Manufacturing Processes*, 31(3), 2016: 233–254. https://doi.org/10.1080/10426914.2015.1025971

[14] S.D. Dhanesh Babu, P. Sevvel, R. Senthil Kumar, V. Vijayan, J. Subramani, Development of Thermo Mechanical Model for Prediction of Temperature Diffusion in Different FSW Tool Pin Geometries During Joining of AZ80A Mg Alloys. *Journal of Inorganic and Organometallic Polymers and Materials*, 31, 2021: 3196–3212. https://doi.org/10.1007/s10904-021-01931-4

[15] S. Celik, R. Cakir, Effect of Friction Stir Welding Parameters on the Mechanical and Microstructure Properties of the Al-Cu Butt Joint. *Metals*, 6(6), 2016: 133. https://doi.org/10.3390/met6060133

[16] V. Msomi, S. Mabuwa, Effect of material positioning on fatigue life of the friction stir processed dissimilar joints. *Materials Research Express*, 7, 2020: 106520. https://doi.org/10.1088/2053-1591/abc18c

[17] H. Kumar, R. Prasad, P. Kumar, Effect of tool pin eccentricity on microstructural and mechanical properties of friction stir processed copper. *Vacuum*, 185, 2021: 110037. https://doi.org/10.1016/j.vacuum.2020.110037

[18] M. Zhai, C. Wu, H. Su, Influence of tool tilt angle on heat transfer and material flow in friction stir welding. *Journal of Manufacturing Processes*, 59, 2020: 98–112. https://doi.org/10.1016/j.jmapro.2020.09.038

[19] A. Ghiasvand, S.M. Noori, W. Suksatan, J. Tomków, S. Memon, H.A. Derazkola, Effect of Tool Positioning Factors on the Strength of Dissimilar Friction Stir Welded Joints of AA7075-T6 and AA6061-T6. *Materials*, 15(7), 2022: 2463. https://doi.org/10.3390/ma15072463

[20] D. García-Navarro, J.C. Ortiz-Cuellar, J.S. Galindo-Valdés, J. Gómez-Casas, C.R. Muñiz-Valdez, N.A. Rodríguez-Rosales, Effects of the FSW Parameters on Microstructure and Electrical Properties in Al 6061-T6- Cu C11000 Plate Joints. *Crystals*, 11(1), 2020: 21. https://doi.org/10.3390/cryst11010021

[21] A. Ghiasvand, M. Kazemi, M.M. Jalilian, H.A. Rashid, Effects of tool offset, pin offset, and alloys position on maximum temperature in dissimilar FSW of AA6061 and AA5086.

International Journal of Mechanical and Materials Engineering, 15, 2020: 6. https://doi.org/10.1186/s40712-020-00118-y

[22] D.O. Bokov, M.A. Jawad, W. Suksatan, M.E. Abdullah, A. Świerczyńska, D. Fydrych, H.A. Derazkola, Effect of Pin Shape on Thermal History of Aluminum-Steel Friction Stir Welded Joint: Computational Fluid Dynamic Modeling and Validation. *Materials*, 14(24), 2021: 7883. https://doi.org/10.3390/ma14247883

[23] H.T. Elmetwally, H.N. SaadAllah, M.S. Abd-Elhady, R.K. Abdel-Magied, Optimum combination of rotational and welding speeds for welding of Al/Cu-butt joint by friction stir welding. *The International Journal of Advanced Manufacturing Technology*, 110, 2020: 163–175. https://doi.org/10.1007/s00170-020-05815-8

[24] S. Chupradit, D.O. Bokov, W. Suksatan, M. Landowski, D. Fydrych, M.E. Abdullah, H.A. Derazkola, Pin Angle Thermal Effects on Friction Stir Welding of AA5058 Aluminum Alloy: CFD Simulation and Experimental Validation. *Materials*, 14(24), 2021: 7565. https://doi.org/10.3390/ma14247565

[25] H.I. Khalaf, R. Al-Sabur, M. Demiral, J. Tomków, J. Łabanowski, M.E. Abdullah, H.A. Derazkola, The Effects of Pin Profile on HDPE Thermomechanical Phenomena during FSW. *Polymers*, 14(21), 2022: 4632. https://doi.org/10.3390/polym14214632

[26] A.S. Bahedh, A. Mishra, R. Al-Sabur, A.K. Jassim, Machine learning algorithms for prediction of penetration depth and geometrical analysis of weld in friction stir spot welding process. *Metallurgical Research and Technology*, 119(3), 2022: 305. https://doi.org/10.1051/metal/2022032

[27] G. Fan, J. Tomków, M.E. Abdullah, H.A. Derazkola, Investigation on polypropylene friction stir joint: effects of tool tilt angle on heat flux, material flow and defect formation. *Journal of Materials Research and Technology*, 23, 2023: 715–729. https://doi.org/10.1016/j.jmrt.2023.01.028

[28] K. Elangovan, V. Balasubramanian, Influences of tool pin profile and welding speed on the formation of friction stir processing zone in AA2219 aluminium alloy. *Journal of Materials Processing Technology*, 200 (1-3), 2008: 163–175. https://doi.org/10.1016/j.jmatprotec.2007.09.019

[29] N. Sharma, A.N. Siddiquee, Z.A. Khan, M.T. Mohammed, Material stirring during FSW of Al–Cu: Effect of pin profile. *Materials and Manufacturing Processes*, 33(7), 2018: 786–794. https://doi.org/10.1080/10426914.2017.1388526

[30] K. Elangovan, V. Balasubramanian, M. Valliappan, Effect of Tool Pin Profile and Tool Rotational Speed on Mechanical Properties of Friction Stir Welded AA6061 Aluminium Alloy. *Materials and Manufacturing Processes*, 23(3), 2008: 251–260. https://doi.org/10.1080/10426910701860723

[31] H. Khodaverdizadeh, A. Heidarzadeh, T. Saeid, Effect of tool pin profile on microstructure and mechanical properties of friction stir welded pure copper joints. *Materials & Design*, 45, 2013: 265–270. https://doi.org/10.1016/j.matdes.2012.09.010

[32] R. Khajeh, H.R. Jafarian, S.H. Seyedein, R. Jabraeili, A.R. Eivani, N. Park, Y. Kim, A. Heidarzadeh, Microstructure, mechanical and electrical properties of dissimilar friction stir welded 2024 aluminum alloy and copper joints. *Journal of Materials Research and Technology*, 14, 2021: 1945–1957. https://doi.org/10.1016/j.jmrt.2021.07.058